Tests of the 2011 Tohoku earthquake source models using free-oscillation data from GOPE

ELIŠKA ZÁBRANOVÁ[1,2], CTIRAD MATYSKA[1*] AND LADISLAV HANYK[1]

1 Department of Geophysics, Faculty of Mathematics and Physics, Charles University in Prague, V Holešovičkách 2, 180 00 Praha 8, Czech Republic

2 Research Institute of Geodesy, Topography and Cartography, Zdiby, Czech Republic

* Corresponding author (ctirad.matyska@mff.cuni.cz)

Received: June 16, 2011; Revised: November 1, 2011; Accepted: January 11, 2012

ABSTRACT

Data from a superconducting gravimeter were obtained from the Geodetic Observatory Pecný (GOPE), Czech Republic, and compared with acceleration data from a broadband seismometer at the same location. We calculated synthetic seismograms for several point- and finite-source fast solutions of the 2011 Tohoku earthquake obtained from surface waves and tested them only against the observed gravity data because of high-noise levels in the low-frequency seismic data. We have obtained a good fit of the synthetic amplitude spectrum with the data up to 1.7 mHz without an additional increase of the moment magnitude M_w. In this aspect, the 2011 Tohoku earthquake was similar to the 2010 Maule earthquake and different from the 2004 Sumatra-Andaman earthquake, where the free-oscillations studies resulted in an increase of the early M_w values. The degree-one mode ${}_3S_1$ dominates the ${}_3S_1$-${}_2S_2$-${}_1S_3$ triplet at the GOPE station.

Keywords: free oscillations of the 2011 Tohoku earthquake, superconducting gravimeter data, source solutions

1. MOTIVATION

The March 11, 2011, Tohoku earthquake together with the 2004 Sumatra-Andaman and the 2010 Maule are the three largest earthquakes recorded during the last decade. Such extraordinary events generate clear signals with a broad frequency content that are strong enough for both detailed structural studies associated with the eigenfrequencies of the Earth and source studies based on modal amplitude analysis (*Park et al., 2005*; *Okal and Stein, 2009*). Because of the complexity of the source region of such events (*Ammon et al., 2005*) their moment magnitude M_w estimates are subject to substantial uncertainty (e.g., *Kanamori, 2006*). The aim of this study is to test several published fast source solutions of the 2011 Tohoku earthquake in the low-frequency range up to 1.7 mHz using data from a superconducting gravimeter at the Geodetic Observatory Pecný (GOPE) (49.9°N, 14.8°E) in the epicentral distance of 81°.

2. GRAVITY AND SEISMIC DATA

The superconducting gravimeter (SG) OSG-050 with the sampling frequency of 1 Hz was installed at the GOPE station in February 2007. The new instrumentation allows the study of a number of geodynamic phenomena towards both the higher frequencies (i.e., free oscillations, long-period seismic waves) and the lower frequencies (e.g., environmental effects, long-period tides). In May 2009 the broadband seismometer (BB) CMG-3TD was installed in a new steel-cased, 60-m deep borehole in the immediate vicinity of the gravimeter. The main characteristics of the BB include 360 s to 50 Hz flat frequency response and the high-stability variant with low self-noise up to 400 s. We have used this collocation of two modern instruments to calculate and compare amplitude spectra of the records from both instruments. Data from the SG were corrected for tides and pressure variations (*Hinderer et al., 2007*). Furthermore, the mean value and linear trend have been removed to eliminate the instrumental drift and residual tidal and air pressure signals. The mass channel of the BB, that directly yields vertical acceleration of the instrument, was used, and the same detrend procedure was applied to the seismic data.

Fig. 1 shows the amplitude spectra of the Tohoku earthquake for 68-hour long records (two upper panels) and 137-hour long records (two bottom panels), respectively, at the GOPE station from both the SG (red line) and the vertical acceleration of the BB (blue line) obtained from the time window starting at March 11, 9:00 UTC. The first panel shows the Fourier amplitude spectrum averaged by the length of the time window, whereas the second panel exhibits the same quantity after applying the Hann filter in the time domain; the same Fourier amplitude spectra obtained for the longer time series are demonstrated in the third and the fourth panels. The application of the Hann filter focuses spectral peaks but, on the other hand, it enhances a relative level of the low-frequency BB noise, because the BB signal of the longest free oscillations is above the noise level only at the beginning of the time series. A substantial increase of the BB noise is thus clearly visible, if the longer time series is employed for spectral analysis. To avoid the problems with the noise at the studied frequency range, we will compare synthetic calculations with the SG signal only, and the data from the BB are shown just to demonstrate a very good mutual agreement of spectral peaks measured by both instruments. The situation at the GOPE station is a good example of the fact that present low-frequency seismology needs supplementary instruments to broadband seismometers; more detailed discussion is in, e.g., *Ferreira et al. (2006)*.

3. SYNTHETIC CALCULATIONS

When spherical harmonic analysis is employed, the equations describing the free oscillations can be written as a system of boundary-value problems for second-order ordinary differential equations. The standard methodology developed for these eigenvalue problems is based on numerical integration of a characteristic equation. The solution of this equation can be numerically problematic, especially when close frequencies need to be separated and/or the skin effect of the eigenfunctions is significant. Our research team has been developing a novel numerical approach, where high-accuracy pseudospectral schemes (*Fornberg, 1996*) are applied to discretize the equations in radial direction. In

such a way, either a matrix eigenvalue problem (in the case of free oscillations) or a system of linear equations (in the case of tidal deformations) is obtained; the main idea of this approach is explained in the Appendix and details can be found in *Zábranová et al. (2009)*. Using numerical libraries for matrix spectral analysis, the eigenfunctions and eigenfrequencies of the fundamental modes are obtained simultaneously. Our calculations of the eigenproblem were performed for the 1-D PREM parameters (*Dziewonski and*

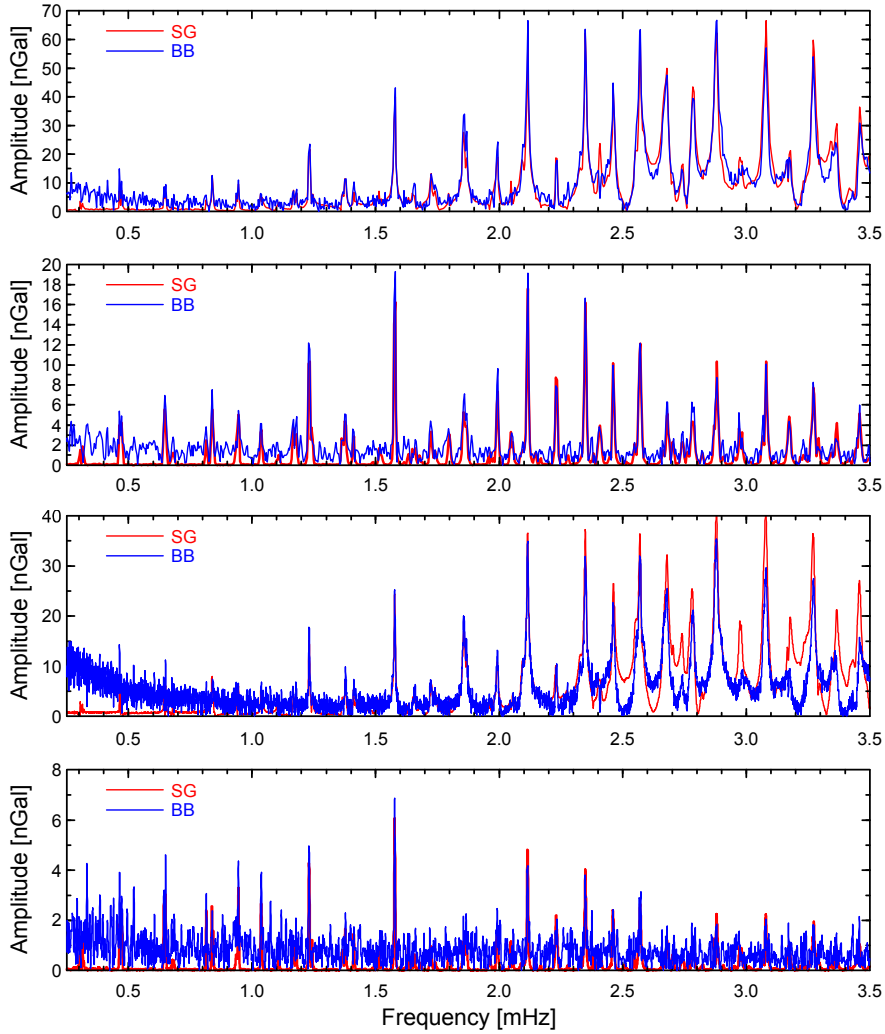

Fig. 1. Vertical acceleration amplitude spectra of the superconducting gravimeter (SG, red line) and the broadband seismometer (BB, blue line) after the March 11, 2011, Tohoku earthquake. The Fourier transform was applied to 68- and 137-hour time series (upper two and bottom two panels, respectively) and the spectrum was averaged over the time window. In the second and the fourth panels the Hann filter was applied before the Fourier transform.

Anderson, 1981) evaluated at the fixed frequency of 1.25 mHz. We also evaluated first-order frequency perturbations of individual modes using Rayleigh's principle and considering a complex perturbation of the isotropic elastic parameters (e.g., *Dahlen and Tromp, 1998*) to obtain the results for the frequency-dependent PREM model.

Moreover, multiplet splitting due to the Coriolis and centrifugal forces and hydrostatic ellipticity were also included following the approach by *Woodhouse and Dahlen (1978)* and *Dahlen and Sailor (1979)*. Note that 1-D structural approximations are still standard tools in low-frequency sources studies (e.g., *Kanamori and Rivera, 2008*). The source and the attenuation have been incorporated into our calculations by means of the formulas of *Dahlen and Tromp (1998)*.

4. RESULTS

Fig. 2 demonstrates the comparisons of the three point-source (PS) and two finite-source (FS) solutions with the SG data. The first source PS1 ($M_w = 9.09$, depth 20 km) is by *Ekström (2011)*, see also *Nettles et al. (2011)*, the second solution PS2 ($M_w = 9.04$, depth 10 km) is the USGS Centroid Moment Tensor Solution (*USGS, 2011a*) and the third model PS3 ($M_w = 9.00$, depth 24 km) is the USGS WPhase Moment Solution (*USGS, 2011b*). The source model FS1, constructed by *Wei and Sladen (2011)*, consists of 252 point sub-sources and its total seismic scalar moment is $M_0 = 5.39 \times 10^{22}$ Nm, which corresponds to $M_w = 9.09$. The last model FS2 is by *Shao et al. (2011)*. It consists of 37050 sub-sources with $M_0 = 5.75 \times 10^{22}$ Nm, which corresponds to slightly higher $M_w = 9.11$.

It is of interest that the PS2 source model clearly yields the strongest synthetic signal for the most of the modes although the moment magnitude M_w of all the source models except PS3 are higher. The reason is that its rake (slip) of 68° is rather anomalous in comparison with the other models. A detailed analysis of individual mode spectra is in Fig. 3, where the data and five synthetic calculations are shown. Moreover, the frequencies of the degenerate multiplets calculated by our code as well as by the Mineos software package (*Masters, 2010*) for the PREM model are written in the panels; the agreement between these two approaches is very good. Individual modes ${}_0S_0$, ${}_0S_2$, ${}_0S_3$, ${}_0S_4$, ${}_0S_5$, ${}_0S_6$, ${}_0S_7$ and ${}_0S_9$, that are clearly separated in the spectrum, are captured by synthetic calculations very well.

The frequencies close to 0.95 mHz, where the mode triplet ${}_3S_1$-${}_2S_2$-${}_1S_3$ occurs, require a special attention, see Fig. 4. The coupling of the modes slightly influences the frequencies (*Zürn et al., 2000*) but we have not incorporated this effect into this study. Further details about the mode coupling can be found in, e.g., *Dahlen and Tromp (1998)* and *Widmer-Schnidrig and Laske (2007)*. The mode ${}_2S_2$ is very weak and can be ignored, similarly to the oscillations studied in *Okal and Stein (2009)*. This is the reason why it is not shown in Fig. 4. The calculated amplitude spectrum of the mode ${}_1S_3$ fits well the data peak at 0.935 mHz, which is caused by the splitting of this mode. However, it strongly underestimates the observed main peak of data at 0.945 mHz. Such a difference can easily be explained by a signal from the mode ${}_3S_1$, that clearly plays a dominant role in this triplet.

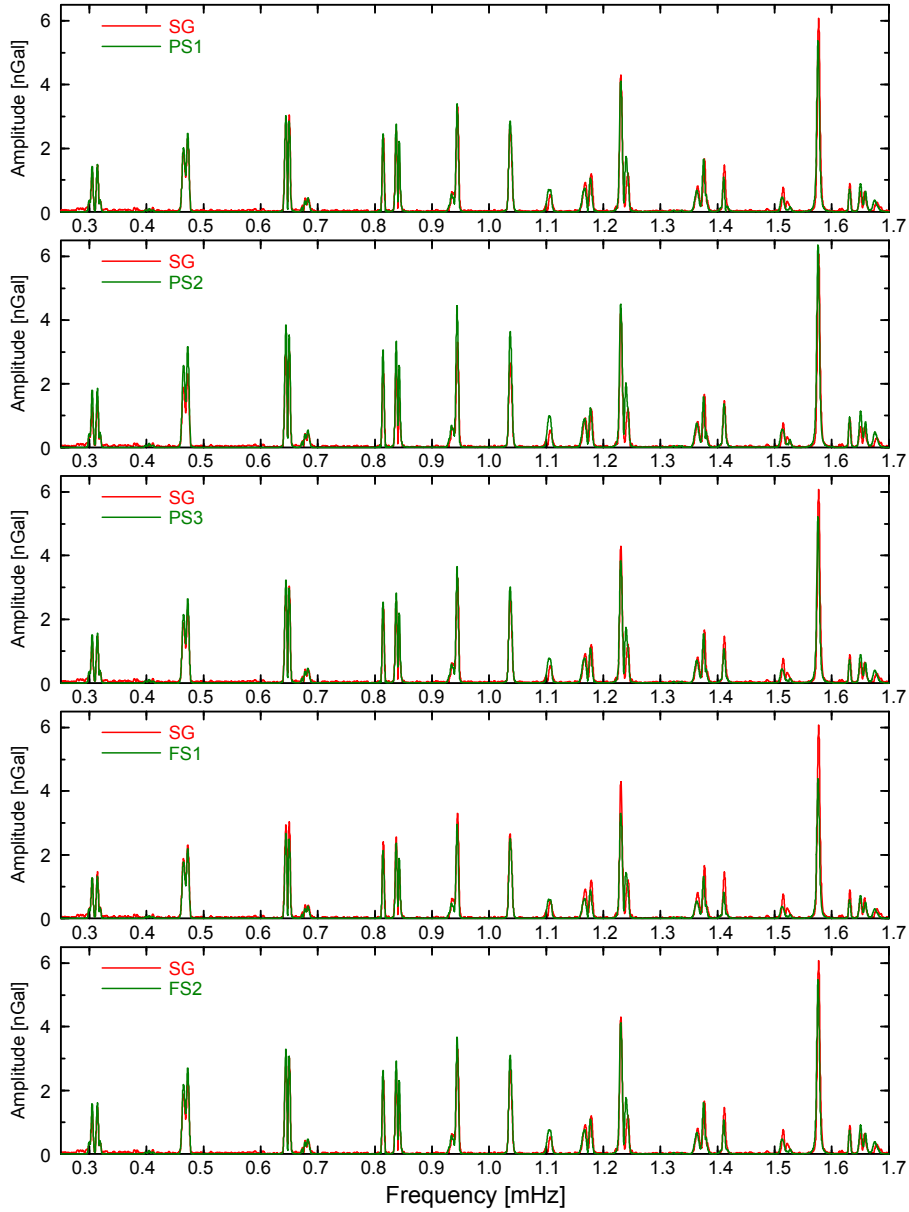

Fig. 2. Vertical acceleration amplitude spectra after the March 11, 2011, Tohoku earthquake. Red lines - superconducting gravimeter, green lines - synthetic calculations for the five fast source solutions: PS1 (*Ekström, 2011*), PS2 (*USGS, 2011a*), PS3 (*USGS, 2011b*); FS1 (*Wei and Sladen, 2011*) and FS2 (*Shao et al., 2011*). The Hann filter and the Fourier transform were applied to 137-hour time series.

In order to evaluate quantitatively the fit of particular modes, we integrated their amplitude spectra over the frequency bands, where synthetic signals of individual modes are effectively non-zero. A relative fit to the data is summarized in Table 1. No source model can be preferred for all the modes but the total power of the studied modes is best fit by the point-source models PS1 and PS3, the geometries of which are very similar but whose magnitudes slightly differ. Nevertheless, the finite source FS1 yields a satisfactory fit for the modes ${}_0S_2$, ${}_0S_3$, ${}_0S_5$, ${}_0S_6$ and the finite source FS2 produces a good fit to the modes ${}_0S_4$, ${}_0S_7$ and ${}_0S_9$. Therefore, one can hardly prefer any of the two solution groups.

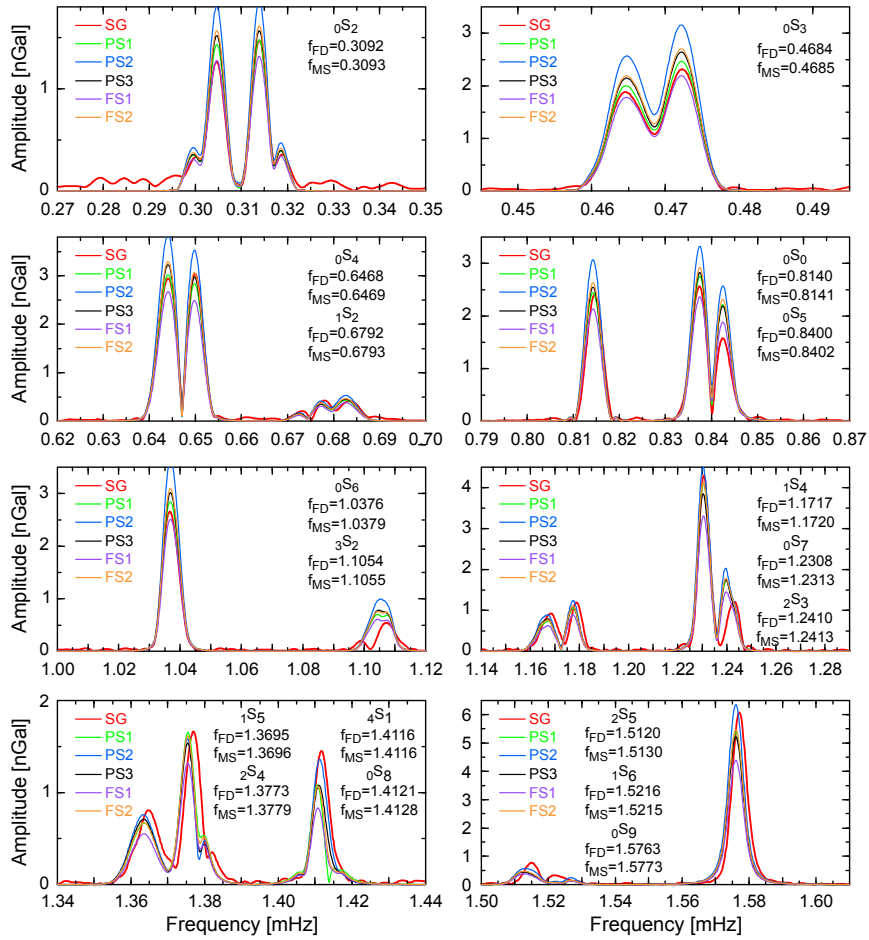

Fig. 3. Vertical acceleration amplitude spectra of fundamental modes after the March 11, 2011, Tohoku earthquake calculated for the three point sources PS1, PS2, PS3 and two finite sources FS1 and FS2 and compared to the observed SG signal. The symbols f_{FD} and f_{MS} denote the unperturbed eigenfrequencies (in mHz) of the spherical PREM model calculated by means of our finite-difference approach and by the Mineos software package (*Masters, 2010*), respectively. The Hann filter and the Fourier transform were applied to 137-hour time series.

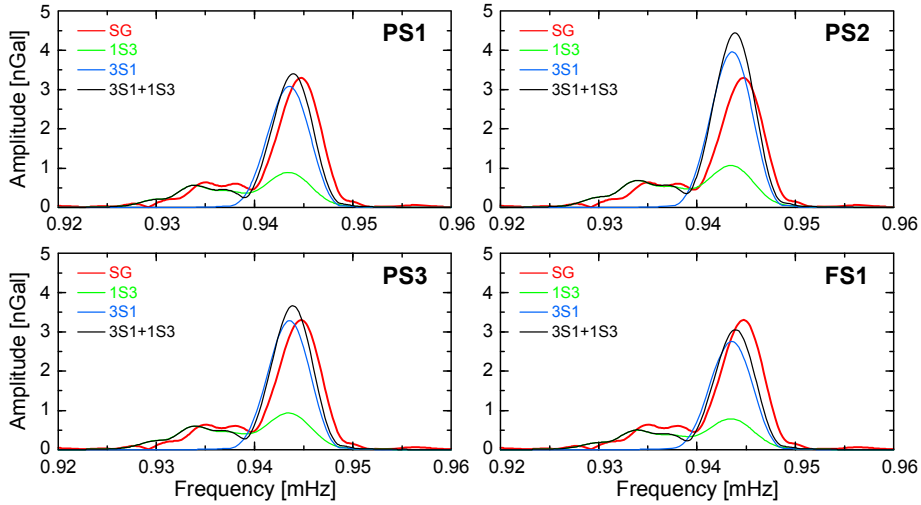

Fig. 4. Vertical acceleration amplitude spectrum of the triplet ${}_3S_{1\text{-}2}S_{2\text{-}1}S_3$ after the March 11, 2011, Tohoku earthquake calculated for the three point sources PS1, PS2, PS3 and the finite source FS1 and compared to the observed SG signal. The synthetic spectrum of the mode ${}_2S_2$ is two orders of magnitude smaller and, therefore, not shown here. The Hann filter and the Fourier transform were applied to 137-hour time series.

Table 1. The relative agreement between the synthetic calculations and the data for the fundamental clearly isolated modes defined by $1-\left|\int_{\delta f} A_g\, df - \int_{\delta f} A_m\, df\right| \Big/ \int_{\delta f} A_g\, df$, where A_m is the amplitude spectrum of models, A_g is the amplitude spectrum of the gravity data and δf is the frequency width of the mode. The last column shows the relative fit after integration over all eight chosen modes for the five fast-source solutions.

Source Model	${}_0S_0$	${}_0S_2$	${}_0S_3$	${}_0S_4$	${}_0S_5$	${}_0S_6$	${}_0S_7$	${}_0S_9$	Total
PS1	0.987	0.951	0.952	0.962	0.839	0.920	0.993	0.923	0.988
PS2	0.729	0.683	0.662	0.792	0.597	0.668	0.882	0.908	0.767
PS3	0.945	0.893	0.879	0.984	0.815	0.889	0.945	0.897	0.969
FS1	0.885	0.933	0.932	0.845	0.999	0.936	0.814	0.755	0.867
FS2	0.911	0.857	0.852	0.960	0.769	0.847	0.991	0.940	0.929

5. CONCLUDING REMARKS

Employing the data from the superconducting gravimeter installed at the GOPE station, we have demonstrated that, in general, the studied 2011 Tohoku earthquake source models obtained from surface waves generate synthetic signals that are in a good agreement with the observed data. Whereas analysis of longest-period normal-mode data of the 2004 Sumatra-Andaman earthquake resulted in an increase of the early M_w values

(*Okal and Stein, 2009*), now the M_w estimates seem to be satisfactory. In this aspect, the 2011 Tohoku earthquake is similar to the 2010 Maule earthquake (*Okal, unpublished results, 2011*). Note that a strong signal of the degree-one mode ${}_3S_1$ is clearly observed in the ${}_3S_{1\text{-}2}S_{2\text{-}1}S_3$ triplet.

Acknowledgments: We thank M. Valko, V. Pálinkáš and V. Plicka for providing us with the data, F. Gallovič for his help with data processing, J. Zahradník and D. A. Yuen for discussion and substantial encouragement, O. Šrámek, J. Velímský and P. Maierová for technical help and anonymous reviewers for their constructive comments and suggestions. This research has been supported by the Grant Agency of the Charles University under the projects No. 2010-141610 and No. 2012-265308 and by the research project MSM 0021620860 of the Czech Ministry of Education, Youth and Sports.

APPENDIX

Spherical harmonic decomposition is commonly used to evaluate eigenfrequencies and eigenfunctions of spherical models. In such a case the momentum and Poisson partial differential equations that describe the spheroidal displacement and changes of the gravity field of a prestressed self-gravitating elastic medium are rewritten into the system of the three second-order ordinary differential equations,

$$\begin{aligned} &\beta U_n'' + \frac{2\beta}{r}U_n' + \left(\frac{4\rho_0 g_0}{r} - 4\pi G\rho^2 - \frac{2\beta+\mu N}{r^2}\right)U_n \\ &-\frac{N}{r}(\lambda+\mu)V_n' + \left(\frac{3\mu+\lambda}{r^2} - \frac{\rho_0 g_0}{r}\right)NV_n - \rho_0 F_n' = -\rho_0\omega_n^2 U_n\,, \end{aligned} \tag{A.1}$$

$$\mu V_n'' + \frac{2\mu}{r}V_n' - \frac{\beta N}{r^2}V_n + \frac{\mu+\lambda}{r}U_n' + \left(\frac{2\beta}{r^2} - \frac{\rho_0 g_0}{r}\right)U_n - \frac{\rho_0}{r}F_n = -\rho_0\omega_n^2 V_n\,, \tag{A.2}$$

$$F_n'' + \frac{2}{r}F_n' - \frac{N}{r^2}F_n + 4\pi G\rho_0\left(U_n' + \frac{2}{r}U_n - \frac{N}{r}V_n\right) = 0\,, \tag{A.3}$$

where r is the radius, ρ_0 is the reference density, G is the Newton gravitational constant, λ and μ are the elastic Lamé parameters, $\beta = \lambda + 2\mu$, n is the degree of the spherical harmonic decomposition, $N = n(n+1)$ and the derivative in the radial direction is denoted by $f' \equiv df/dr$. U_n, V_n and F_n are the coefficients of spherical harmonic expansions representing the spheroidal displacement vector and incremental gravitational potential, and ω_n are the angular frequencies of free oscillations for a fixed n.

We follow the finite-difference approach designed by *Fornberg (1996)*, where a pseudospectral accuracy of finite differences is reached by evaluating the unknowns at the extrema of the Chebyshev polynomials. Note that in layered models, such as the PREM, an independent Chebyshev grid is applied to each layer. Eqs.(A.1)–(A.3), including boundary conditions, can then be rewritten into the unified matrix form,

$$\left(\mathbf{P}^{-1}\cdot\mathbf{R}\right)\cdot\boldsymbol{Y}=-\frac{1}{\omega^2}\boldsymbol{Y}\,, \tag{A.4}$$

where **P** and **R** are the matrices of coefficients depending on model parameters and discretization, ***Y*** are eigenfunctions composed of the discrete values U_n, V_n and F_n and $-1/\omega^2$ are the eigennumbers. The discrete forms of the matrices **P**, **R** and the vector ***Y*** are derived in *Zábranová et al. (2009)*.

The PREM model is frequency dependent and its parameters that appear in the formulas above are evaluated for a fiducial frequency $\bar{\omega}$. Following *Dahlen and Tromp (1998)*, the slight shift of an individual mode frequency ω_0 caused by isotropic anelasticity can be incorporated by the formula

$$\omega=\omega_0+\frac{1}{\pi}\omega_0 Q^{-1}\ln\frac{\omega_0}{\bar{\omega}}\,, \tag{A.5}$$

where Q is the quality factor.

Splitting frequency perturbations of an isolated multiplet due to the effects of the Earth's rotation and hydrostatic ellipticity can be expressed as

$$\delta\omega_m=\omega\left(a+bm+cm^2\right), \tag{A.6}$$

where m, $-n\le m\le n$, is the order. The term b arises from the first-order effect of the Coriolis force and the terms a and c arise from ellipticity and second-order effects of rotation.

The vertical acceleration of an instrument can be written in the form

$$\boldsymbol{a}\left(\boldsymbol{x},t\right)=\sum_{nlm}A_{nlm}\left(\boldsymbol{x}\right)\exp\left[\mathrm{i}_l\omega_n\left(1+a+bm+cm^2\right)t-{}_l\gamma_n t\right], \tag{A.7}$$

where the sum is over all multiplets defined by degrees n and overtone numbers l. The coefficients A_{nlm} are given by the moment tensor, a source-receiver geometry and the eigenfunctions, and ${}_l\gamma_n$ is the decay rate of each multiplet.

References

Ammon C.J., Ji C., Thio H-K., Robinson D., Ni S., Hjorleifsdottir V., Kanamori H., Lay T., Das S., Helmberger D., Ichinose G., Polet J. and Wald D., 2005. Rupture process of the 2004 Sumatra-Andaman earthquake. *Science*, **308**, 1133–1139.

Dahlen F.A. and Tromp J., 1998. *Theoretical Global Seismology*. Princeton University Press, Princeton.

Dahlen F.A. and Sailor R.V., 1979. Rotational and elliptical splitting of the free oscillations of the Earth. *Geophys. J. R. Astr. Soc.*, **58**, 609–623.

Dziewonski A.M. and Anderson D.L., 1981. Preliminary reference Earth model. *Phys. Earth Planet. Inter.*, **25**, 297–356.

Ekström G., 2011. http://earthquake.usgs.gov/earthquakes/eqinthenews/2011/usc0001xgp/neic_c0001xgp_gcmt.php.

Ferreira A.M.G., d'Oreye N.F., Woodhouse J.H. and Zürn W., 2006. Comparison of fluid tiltmeter data with long-period seismograms: Surface waves and Earth's free oscillations. *J. Geophys. Res.*, **111**, B11307.

Fornberg B., 1996. *A Practical Guide to Pseudospectral Methods*. Cambridge University Press, New York.

Hinderer J., Crossley D. and Warburton R.J., 2007. *Gravimetric methods - superconducting gravity meters*. In: Herring T. (Ed.), *Treatise on Geophysics, Vol.3, Geodesy*. Elsevier, Amsterdam, The Netherlands, 66–122.

Kanamori H., 2006. Lessons from the 2004 Sumatra-Andaman earthquake. *Phil. Trans. R. Soc. A*, **364**, 1927–1945.

Kanamori H. and Rivera L., 2008. Source inversion of Wphase: speeding up seismic tsunami warning. *Geophys. J. Int.*, **175**, 222–238.

Masters G., 2010. *Mineos Package*. http://geodynamics.org/cig/software/mineos.

Nettles M., Ekström G. and Koss H.C., 2011. Centroid-moment-tensor analysis of the 2011 off the Pacific coast of Tohoku Earthquake and its larger foreshocks and aftershocks. *Earth Planets Space*, **63**, 519–523.

Okal E.A. and Stein S., 2009. Observations of ultra-long period normal modes from the 2004 Sumatra-Andaman earthquake. *Phys. Earth Planet. Inter.*, **175**, 53–62.

Park J., Song T.-R.A., Tromp J., Okal E., Stein S., Roult G., Clevede E., Laske G., Kanamori H., Davis P., Berger J., Braitenberg C., van Camp M., Lei X., Sun H., Xu H. and Rosat S., 2005. Earth's free oscillations excited by the 26 December 2004 Sumatra-Andaman earthquake. *Science*, **308**, 1139–1144.

Shao G., Li X. and Ji C., 2011. http://www.geol.ucsb.edu/faculty/ji/big_earthquakes/2011/03/0311_v3/Honshu.html.

USGS, 2011a. http://earthquake.usgs.gov/earthquakes/eqinthenews/2011/usc0001xgp/neic_c0001xgp_cmt.php.

USGS, 2011b. http://earthquake.usgs.gov/earthquakes/eqinthenews/2011/usc0001xgp/neic_c0001xgp_wmt.php.

Wei S. and Sladen A., 2011. http://www.tectonics.caltech.edu/slip_history/2011_tohoku-oki-tele.

Widmer-Schnidrig R. and Laske G., 2007. Theory and observations - normal modes and surface wave measurements. In: Romanowicz B.A. and Dziewonski A.M. (Eds.), *Treatise on Geophysics, Vol.1, Seismology and the Structure of the Earth*. Elsevier, Amsterdam, The Netherlands, 67–125.

Woodhouse J.H. and Dahlen F.A., 1978. The effect of a general aspherical perturbation on the free oscillations of the Earth. *Geophys. J. R. Astr. Soc.*, **53**, 335–354.

Zábranová E., Hanyk L. and Matyska C., 2009. Matrix pseudospectral method for elastic tides modeling. In: Holota P. (Ed.), *Mission and Passion: Science*. Czech National Committee of Geodesy and Geophysics, Prague, 243–260, http://geo.mff.cuni.cz/documents/2009-Zabranova.pdf.

Zürn W., Laske G., Widmer-Schnidrig R. and Gilbert F., 2000. Observation of Coriolis coupled modes below 1 mHz. *Geophys. J. Int.*, **143**, 113–118.